# Amorphous silica modeled with truncated and screened Coulomb interactions: A molecular dynamics simulation study

Antoine Carré
*Institut für Physik, Johannes Gutenberg-Universität Mainz, Staudinger Weg 7, 55099 Mainz, Germany; Laboratoire de Colloïdes, Verres et Nanomatériaux, UMR 5587, Université Montpellier II and CNRS, 34095 Montpellier, France*

Ludovic Berthier
*Laboratoire de Colloïdes, Verres et Nanomatériaux, UMR 5587, Université Montpellier II and CNRS, 34095 Montpellier, France; and Joint Theory Institute, Argonne National Laboratory, Chicago, Illinois 60439; and University of Chicago, Chicago, Illinois 60637*

Jürgen Horbach
*Institut für Physik, Johannes Gutenberg-Universität Mainz, Staudinger Weg 7, 55099 Mainz, Germany and Institut für Materialphysik im Weltraum, Deutsches Zentrum für Luft-und Raumfahrt, 51147 Köln, Germany*

Simona Ispas and Walter Kob
*Laboratoire de Colloïdes, Verres et Nanomatériaux, UMR 5587, Université Montpellier II and CNRS, 34095 Montpellier, France*

(Received 3 July 2007; accepted 6 August 2007; published online 21 September 2007)

We show that finite-range alternatives to the standard long-range pair potential for silica by van Beest *et al.* [Phys. Rev. Lett. **64**, 1955 (1990)] might be used in molecular dynamics simulations. We study two such models that can be efficiently simulated since no Ewald summation is required. We first consider the Wolf method, where the Coulomb interactions are truncated at a cutoff distance $r_c$ such that the requirement of charge neutrality holds. Various static and dynamic quantities are computed and compared to results from simulations using Ewald summations. We find very good agreement for $r_c \approx 10$ Å. For lower values of $r_c$, the long-range structure is affected which is accompanied by a slight acceleration of dynamic properties. In a second approach, the Coulomb interaction is replaced by an effective Yukawa interaction with two new parameters determined by a force fitting procedure. The same trend as for the Wolf method is seen. However, slightly larger cutoffs have to be used in order to obtain the same accuracy with respect to static and dynamic quantities as for the Wolf method. © *2007 American Institute of Physics*. [DOI: 10.1063/1.2777136]

## I. INTRODUCTION

Silica ($SiO_2$) is the prototype of a glass former that exhibits a tetrahedral network structure. It is the basic oxidic component of many minerals and technological glasses. In recent years, molecular dynamics (MD) computer simulations have provided valuable insight into static and dynamic properties of amorphous and crystalline silica.[1–25] In a classical MD simulation, the interactions between the atoms are described by an effective potential where, different from *ab initio* approaches, the electronic degrees of freedom are not taken into account explicitly. In many of the aforementioned MD studies, the so-called van Beest–Kramer–Van Santen (BKS) potential[26] has been used. Although it is a standard pair potential, it yields good agreement with experimental data. However, it contains a long-range Coulomb interaction term and thus the computation of energies and forces is very expensive, in particular, for large systems. Therefore, it is important to know whether silica can also be modeled by a potential with a *finite* range.

The classical approach to evaluate Coulomb energies and forces in a simulation is the Ewald summation method where the sum over all Coulomb interactions is decomposed into a real space and a Fourier part.[27–29] For a three-dimensional $N$ particle system with periodic boundary conditions in all three spatial directions, Ewald method yields a $N^{3/2}$ scaling for the computational load.[29,30] Even worse is the case of a quasi-two-dimensional slab geometry for which Ewald method exhibits a $N^2$ scaling.[31] There are modifications of the Ewald method such as particle-particle particle-mesh methods[32,33] (PPPMs) that yield a scaling proportional to $N \log N$, but these methods cannot be implemented as efficiently as in the three-dimensional case for the quasi-two-dimensional geometry.[34] A scaling better than $\mathcal{O}(N \log N)$ can be reached by means of multipole methods.[35] However, these methods introduce a large computational overhead such that their use is only reasonable for a very large number of particles, say $N > 10^5$.[36]

Apart from the case of quasi-two-dimensional geometries, there are other applications where it is difficult to handle long-range Coulomb interactions. For instance, the calculation of transport coefficients such as the shear viscosity via Green-Kubo relations is in general more complicated and less efficient when Ewald sums have to be considered.[28] This is also the case for Monte Carlo (MC) simulations.

 

When using Ewald summation (or also PPPM) in MC simulations, the full Fourier part of the Coulomb energy must be evaluated after each particle displacement by summing over $N$ terms and $N_k$ different wave vectors used in the Ewald summation. Note that this is much worse than for MD where the sum over wave vectors can at least be used to compute the force over all $N$ particles, while the energy must be recomputed after each single move in MC simulations.

For all these reasons, a reliable finite-range pair potential to simulate silica is highly desirable. In this paper, we address this issue by making the assumption that, due to screening effects, the long-range Coulomb interactions in typical ionic systems can, in fact, be truncated.[37] However, a cutoff distance $r_c$ for a $r^{-1}$ potential cannot be introduced in a similar manner as for a short-range potential since a truncated spherical summation over pairwise $r^{-1}$ Coulomb terms leads to a violation of charge neutrality. In order to circumvent this problem, Wolf *et al.*[37,38] have introduced a simple correction term in the truncated Coulomb sums that recovers the requirement of charge neutrality. The Wolf method [37–39] has been used in recent simulation studies, e.g., for quasi-two-dimensional geometries,[40] in MC simulations,[41] or for dipolar fluids.[42] Of course, it is *a priori* not clear how large the cutoff radius $r_c$ has to be in order to correctly reproduce the static and dynamic properties of the original model with long-range Coulomb interactions. We have carefully studied this issue using MD simulations of amorphous silica based on the BKS potential. We show that a cutoff of about 10 Å is necessary to obtain good agreement with the initial long-range model on a quantitative level. This indicates that, due to screening effects, amorphous silica can indeed be described by an effective potential of finite range. Therefore, in our second approach we reparametrize the Coulomb term of the BKS potential by replacing it by a screened Coulomb (Yukawa) potential with two new parameters. The parametrization of this Yukawa potential is achieved by a force fitting procedure based on previous MD simulations of BKS silica.[4] This alternative procedure is of course more involved than the simpler Wolf truncation, as the new pair potential must be carefully parametrized.

The paper is organized as follows. In Sec. II, we introduce the truncated and screened Coulomb potentials studied in this work, and we describe how the free parameters are fixed. In Sec. III, we use a given set of fixed parameters and compare in detail static and dynamic properties of the original long-range BKS model and the two finite-range alternatives suggested in this paper. We present our conclusions in Sec. IV.

## II. TWO FINITE-RANGE ALTERNATIVES

### A. The original long-range BKS model

The functional form of the BKS potential is[26]

$$\phi_{\alpha\beta}^{\mathrm{BKS}}(r) = q_\alpha q_\beta e^2 V_C(r) + A_{\alpha\beta}\exp(-B_{\alpha\beta}r) - \frac{C_{\alpha\beta}}{r^6}, \qquad (1)$$

where $\alpha, \beta \in [\mathrm{Si}, \mathrm{O}]$, and $r$ is the distance between the ions of type $\alpha$ and $\beta$. The values of the constants $q_\alpha$, $q_\beta$, $A_{\alpha\beta}$, $B_{\alpha\beta}$, and $C_{\alpha\beta}$ can be found in Ref. 26. For the sake of computational efficiency the short-range part of the potential was truncated and shifted at 5.5 Å.[2] This truncation also has the benefit of improving the agreement between simulation and experiment with respect to the density of the amorphous glass at low temperatures.[2,4] Finally, the function

$$V_C(r) = \frac{1}{r} \qquad (2)$$

is the Coulomb long-range term which will be further approximated by finite-range potentials. The other terms in Eq. (1) will be unchanged.

In numerical simulations using periodic boundary conditions, the Coulombic part of the potential energy $E_{\mathrm{coul}}$ is given by the following formula:

$$E_{\mathrm{coul}} = \frac{1}{2}\sum_{\mathbf{n}\in\mathbf{Z}^3}\sum_{\substack{i,j=1 \\ i\neq j \text{ for } \mathbf{n}=0}}^{N} \frac{q_i q_j e^2}{|\mathbf{r}_{ij}+\mathbf{n}L|}. \qquad (3)$$

Here, $\mathbf{r}_{ij}=\mathbf{r}_i-\mathbf{r}_j$ is the distance vector between particle $i$ and particle $j$. The sum over $\mathbf{n}$ takes into account the interactions of a particle $i$ with all the replicated image particles (including the images of particle $i$). Moreover, it is only conditionally convergent, i.e., the value of the sum depends on the order by which the terms are summed up. An efficient method to circumvent these problems is provided by the Ewald summation technique. However, finite-range alternatives to Ewald sums are very desirable, as outlined in the Introduction. The analysis of such alternatives is the principal aim of this paper.

We shall analyze the ability of finite-range potentials to reproduce the behavior of the original BKS model by comparing the results of molecular dynamics simulations of the new potentials against results employing Ewald sums. The latter results are taken from previously published works[4,23] and they will be labeled "Ewald simulations" hereafter. Most of the Ewald simulations were performed with $N=1008$ particles, at the density of 2.37 $\mathrm{g/cm^3}$, with Ewald parameters ($\alpha$ and $N_k$) optimized as in Ref. 2. In particular, the real space part of the Coulomb force is truncated at 10.17 Å, and we take the results of these simulations as representatives of the behavior of the "real" Coulomb potential. We know, however, that finite size effects are present for this system size, and we borrow additional data from the $N=8016$ particle simulations from Ref. 4 when necessary.

### B. Truncation using the Wolf method

As proposed in Refs. 37–39, the $V_C(r)$ term in the BKS potential (1) may be approximated by the following form:

$$V_W(r) = \left(\frac{1}{r}-\frac{1}{r_c}\right) + \frac{1}{r_c^2}(r-r_c), \quad r<r_c, \qquad (4)$$

while $V_W(r\geqslant r_c)=0$. The potential [Eq. (4)] is a finite-range potential: Only particles separated by distances smaller than $r_c$ interact. Such a potential becomes computationally extremely useful when system sizes that are much larger than $r_c$ are studied. However, Wolf's main point is that reasonable values of $r_c$ can lead to numerically accurate results.[37] The

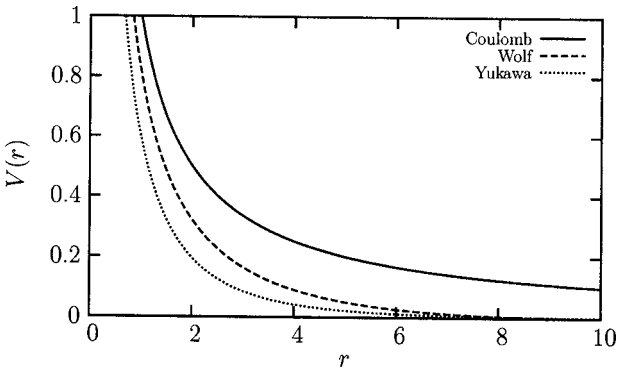


FIG. 1. Comparison of the pure $1/r$ Coulomb interaction, the Wolf truncation using Eq. (4) for $r_c=10.17$ Å, and the Yukawa potential in Eq. (7), for $D_Y=1.07$, $\Delta=5.649$ Å, and $r_c=10.17$ Å.

fact that this is by no means a trivial statement can be appreciated in Fig. 1 which compares the initial Coulomb interaction in Eq. (1) to the expression given by Eq. (4). Both potentials are very different, and the truncation should in principle have a drastic effect. Indeed previous naive truncation attempts have been shown to produce quantitatively inaccurate results.[20] We shall demonstrate, however, that the Wolf method performs well in the case of liquid silica.

The truncated form of the potential [Eq. (4)] can be justified as follows. Wolf[37] showed that the main error made when imposing naively a finite distance cutoff to a $1/r$ potential stems from the fact that a sphere of radius $r_c$ centered around a particle is in general charged, so that its interaction with the rest of the system is not negligible. He proposed to approximate this interaction by using the potential

$$V(r)=\frac{1}{r}-\frac{1}{r_c}, \quad r<r_c,$$

which amounts to screening completely the charge contained in the sphere by placing the opposite charge on its surface. This form is also natural from the computational point of view: Truncated potentials in molecular dynamics simulations are always shifted to avoid energy discontinuities at the cutoff, $V(r=r_c)=0$. Although the shift is sufficient to compute the energy, which was the initial problem considered by Wolf,[37] this potential is not well suited for MD simulations since the forces are discontinuous at $r_c$.[38] Hence, the second term is added in Eq. (4), as suggested in Ref. 39.

We have performed MD simulations with the BKS model [Eq. (1)] where we have approximated the $1/r$ Coulomb interaction term by the Wolf formula [Eq. (4)]. For the cutoff $r_c$ in Eq. (4), three different values have been chosen, namely, $r_c=6.0$, 8.0, and 10.17 Å. Note that a cutoff of $r_c=10.17$ Å has also been used for the real space part of the Ewald sums in our simulations using the original BKS potential.[23] For a system of $N=1008$ particles, the gain in CPU time with the Wolf method is a factor of 2 for $r_c=10.17$ Å. Although this speedup is not that impressive, one should keep in mind that the Wolf method is also well suited for problems where Ewald sums become very inefficient, e.g., for quasi-two-dimensional geometries, for MC simulations, or for large systems (see Introduction). In addition the

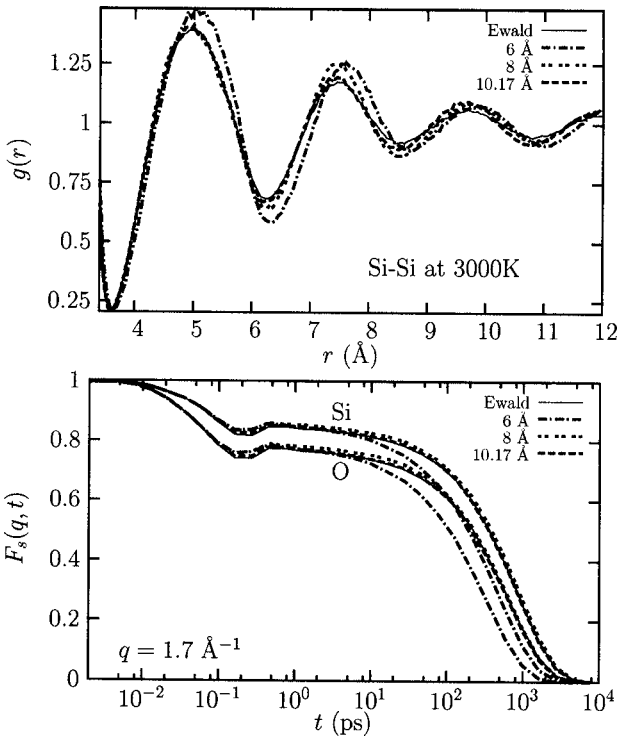


FIG. 2. Top: Influence of the Wolf cutoff on the Si–Si pair correlation function for large distance. Bottom: Influence of the Wolf cutoff on the time dependence of the self-intermediate scattering function for both Si (top curves) and O (bottom curves). Both panels are for $T=3000$ K.

structure of the code and the calculations of physical quantities become much simpler if the potential has only a finite range.

Equilibrated configurations from simulations with Ewald sums[23] were used as starting configurations for the MD simulations with the Wolf method at each temperature between 3000 and 6100 K. The considered temperatures were 3000, 3100, 3250, 3400, 3580, 3760, 4000, 4300, 4700, 5200, and 6100 K, i.e., the same values as the ones considered in Ref. 4. As in Refs. 4 and 23, the velocity form of the Verlet algorithm[28] was used to integrate the equations of motion with a time step of 1.6 fs. Equilibration runs were made by coupling the system to a stochastic heat bath before performing productions runs in the microcanonical ensemble. During the equilibration, we detect no systematic drift of the energy for $r_c=10.17$ Å, which is a first indication that Ewald and Wolf methods should yield very close results for this cutoff value. During microcanonical simulations at 3000 K, the drift in the total energy is comparable in amplitude to the one observed when using Ewald summations. Therefore, we follow Ref. 4 and rescale velocities every $10^6$ time steps to maintain the total energy constant.

We have analyzed a number of static and dynamic quantities (see Sec. III), and we find that deviations between Wolf and Ewald methods become more pronounced when temperature decreases, and, of course, when the cutoff value decreases. This temperature evolution suggests that charges are more efficiently screened at high temperatures in amorphous silica when the system is more disordered.

In Fig. 2, we present selected static and dynamic results

at $T=3000$ K for different values of the cutoff. As a dynamic quantity, we show the self part of the intermediate scattering function,[43]

$$F_s(\mathbf{q},t)=\frac{1}{N_\alpha}\sum_{j=1}^{N_\alpha}\langle e^{i\mathbf{q}\cdot(\mathbf{r}_j(t)-\mathbf{r}_j(0))}\rangle, \tag{5}$$

where $\mathbf{r}_j(t)$ is the position of particle $j$ of type $\alpha$ at time $t$. As a representative structural quantity we show the pair correlation function $g_{\alpha\beta}(r)$ (with $\alpha,\beta=\mathrm{Si,O}$),

$$g_{\alpha\beta}(r)=\frac{V}{N_\alpha(N_\beta-\delta_{\alpha\beta})}\left\langle\sum_{i=1}^{N_\alpha}\sum_{j=1}^{N_\beta}\frac{1}{4\pi r^2}\delta(r-|\mathbf{r}_i-\mathbf{r}_j|)\right\rangle, \tag{6}$$

where $V$ is the total volume of the system and $N_\alpha$ the number of particles of type $\alpha$. In Fig. 2, the function $g_{\mathrm{SiSi}}(r)$ is shown for $r\geqslant 4$ Å since the Si–Si correlations exhibit the largest effects with respect to the cutoff $r_c$, at large distance.

For $r_c=6$ Å, deviations between Ewald and Wolf methods are obvious. Self-intermediate scattering functions decay faster with Wolf than with Ewald method, and the positions of the second and third peaks in the pair correlation function $g_{\mathrm{SiSi}}(r)$ arise at different values in the two methods. For $r_c=8$ Å, the situation is already much better since structural relaxation occurs at the correct time scale, and oscillations in $g_{\mathrm{SiSi}}(r)$ are in phase with the corresponding Ewald result. However, a closer inspection of the data shows that the plateau value in the self-intermediate scattering function is not correctly reproduced and the amplitude of the oscillations in $g_{\mathrm{SiSi}}(r)$ is too large at large distance. For $r_c=10.17$ Å, the agreement with the Ewald simulation is almost perfect both for statics and dynamics. The height of the plateau in $F_s(q,t)$ is now correct and the amplitude of the oscillations in $g_{\mathrm{SiSi}}(r)$ is very close to those of the Ewald result. Looking very closely at the data, however, a few deviations remain. The oscillations in $g_{\mathrm{SiSi}}(r)$ at large distances are still too pronounced, meaning that long-range order in the liquid is slightly more pronounced when using Wolf's method (see also the discussion concerning the results shown in Fig. 6). The amplitude of the small dip in $F_s(q,t)$ around $t\sim 1$ ps is much smaller for $r_c=6$ and 8 Å and remains a bit too small for $r_c=10.17$ Å, although it is only a tiny difference in the latter case.

The influence of the cutoff and convergence toward the Ewald results is further confirmed by the behavior of the pressure, which will be studied in more detail in Sec. III. In fact, we find that the pressure represents a very sensitive test for the choice of $r_c$. For $T=3000$ K, we find $P\approx -3.2,-0.11$, and 0.83 GPa for $r_c=6,8$, and 10.17 Å, respectively, while $P\approx 0.89$ GPa using Ewald sums for the same number of particles.

From the results described in this section we decide therefore that $r_c=10.17$ Å is a good compromise between a small cutoff which improves computational efficiency and a very large cutoff which matches best the behavior observed in simulations using Ewald sums. In Sec. III, we shall present a more extensive set of static and dynamic data for $r_c=10.17$ Å and we will show that this produces a physical behavior in satisfying quantitative agreement with simulations using Ewald sums.

### C. Yukawa screening

The replacement of the $1/r$ interaction by a screened Coulomb interaction has been proposed in several recent simulation studies of various atomistic systems (see, e.g., Refs. 19, 20, 39, and 44 and references therein). In these studies, screened Coulomb or Yukawa potentials have been considered as alternatives to the Wolf method presented above.

In the present work, we reparametrize the BKS potential by replacing $V_C(r)$ term in Eq. (1) by a Yukawa interaction term of the following form:

$$V_Y(r)=D_Y\frac{\exp(-r/\Delta)}{r}, \tag{7}$$

which introduces the amplitude $D_Y$ and the screening length $\Delta$ as new parameters. Note that in Eq. (7) the same parameters $D_Y$ and $\Delta$ are used for Si–Si, Si–O, and O–O interactions. The shape of the Yukawa interaction is compared to the one of the Wolf and Coulomb terms in Fig. 1.

Our determination of $D_Y$ and $\Delta$ was based on previous MD simulations for a system of 8016 particles using the BKS potential.[4] At each temperature in the interval of $6100\ \mathrm{K}\leqslant T\leqslant 2750$ K (see Ref. 4 for the considered values) the parameters $D_Y$ and $\Delta$ are fitted such that the forces on each particle of the BKS configurations are optimally reproduced by the new potential. More precisely, the fitting procedure was based on the following $\chi^2$ function:

$$\chi^2=\left\langle\frac{1}{3N}\sum_{\alpha=\mathrm{Si,O}}\frac{1}{\sigma_\alpha^2}\sum_{i=1}^{N_\alpha}|\mathbf{F}_i^{\mathrm{BKS}}-\mathbf{F}_i^{Y}|^2\right\rangle, \tag{8}$$

where $\mathbf{F}_i^{\mathrm{BKS}}$ and $\mathbf{F}_i^{Y}$ denote the total forces on the particle $i$ for the original BKS potential and the new BKS potential modified by the screened Coulomb term [Eq. (7)], respectively. The $\sigma_\alpha$ represents the standard deviation of the BKS force distribution for Si and O particles. We find $\sigma_{\mathrm{Si}}(T=6100\ \mathrm{K})=4.427\,614$ eV/Å, $\sigma_{\mathrm{O}}(T=6100\ \mathrm{K})=3.674\,404$ eV/Å, $\sigma_{\mathrm{Si}}(T=2750\ \mathrm{K})=3.235\,584$ eV/Å, and $\sigma_{\mathrm{O}}(T=2750\ \mathrm{K})=2.632\,564$ eV/Å. The brackets $\langle\cdots\rangle$ denote an average over different samples (i.e., BKS configurations).

It is important to note that if we use the ansatz in Eq. (7) with $\Delta$ and $D_Y$ as the only two free parameters, the function $\chi^2$ could only be minimized by approaching the limits of $\Delta=\infty$ and $D_Y=1$, thus reproducing the original Coulomb interaction. Therefore, we have to introduce a third parameter, namely, a cutoff distance $r_c$ above which the potential $V_Y(r)$ is set to zero. Thus, we shall first fix the value of the cutoff $r_c$, and then determine the best set of parameters for $D_Y$ and $\Delta$ to minimize the function in Eq. (8). This procedure can then be repeated for different values of the cutoff $r_c$ and for different temperatures. The outcome of this study will be the suggestion of an "optimal" set of parameters ($r_c$, $D_Y$, and $\Delta$) that can be used to study the properties of silica at various temperatures.

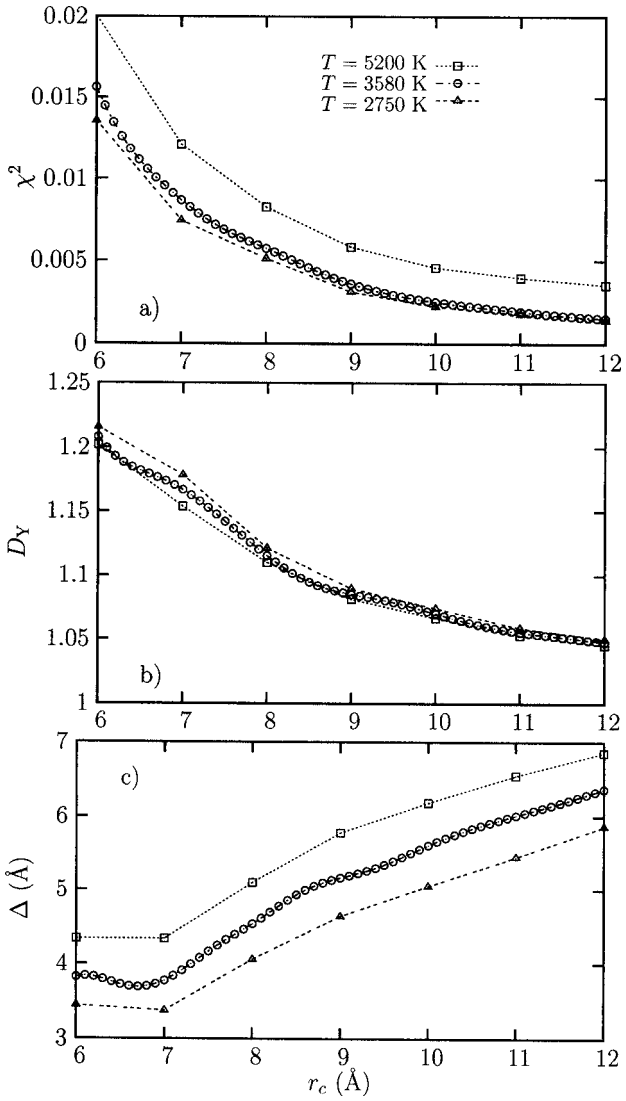


FIG. 3. Dependence of the $\chi^2$ (a), prefactor $D_Y$ (b), and screening length Δ (c) of the Yukawa potential [Eq. (7)] as functions of the cutoff $r_c$ for the three indicated temperatures.

Note that the use of a cutoff in the potential [Eq. (7)] implies a discontinuity of the forces at $r_c$. As already mentioned in the previous section, this is not useful for MD simulations since it leads to an energy drift in microcanonical simulation runs. Therefore, we have multiplied the *forces* $\mathbf{F}_i^Y$ by the function

$$f(r) = \exp\left(-\frac{h^2}{(r-r_c)^2}\right), \quad r < r_c, \tag{9}$$

which makes the forces continuous at $r_c$. The constant $h$ was set to 2.0 Å.

The $\chi^2$ function (8) was minimized by means of the Levenberg-Marquardt algorithm,[45] which is essentially a conjugate gradient scheme for nonlinear fitting problems. As shown in Fig. 3(a), $\chi^2$ decreases when temperature decreases, although the temperature dependence is relatively weak. It also decreases relatively quickly as a function of the cutoff radius $r_c$ for the Yukawa potential. Empirically we find that the data at $T=3580$ K in Fig. 3(a) can be well described with a power law behavior, $\chi^2(r) \propto 1/r^{3.4}$. It is indeed expected that $\chi^2$ vanishes at large $r_c$ since in the limit of $r_c \to \infty$, the original Coulomb potential should be recovered. Therefore, the screening length Δ should diverge for large values of $r_c$ while the amplitude $D_Y$ should approach 1, as confirmed by our numerical results in Figs. 3(b) and 3(c).

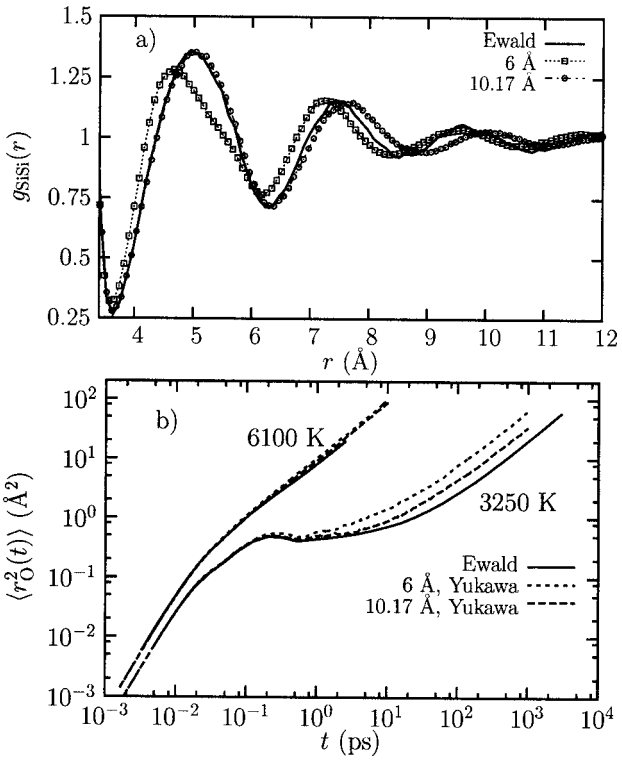


FIG. 4. Influence of the cutoff $r_c$ for the Yukawa potential on the Si–Si pair correlation function at $T=3250$ K (a) and on the mean-squared displacement for the silicon atoms (b) for the indicated temperatures.

Whereas the temperature dependence of $D_Y$ is relatively weak, the screening length Δ decreases significantly with decreasing temperature, which can be understood as follows. Physically, the value of Δ obtained using the minimization procedure results from a compromise. On the one hand, a large screening length Δ should be used to recover the "bare" Coulomb potential. On the other hand, the introduction of a finite distance cutoff $r_c$ produces large errors due to incorrect charge balance.[37] In the present scheme, this is compensated by screening more strongly the Coulomb interaction by using a smaller screening length Δ. Thus the results in Fig. 3(c) indicate that that charge neutrality is best satisfied, for a fixed cutoff value $r_c$, when temperature is higher, so that a larger screening length Δ can be used at high temperature. In turn, this suggests that charges in amorphous silica are screened on a smaller length scale when temperature is high that is, when the system is more disordered. The same conclusion was reached in Sec. II B.

It is also remarkable that the evolution of $D_Y$ and Δ with the cutoff is not completely trivial but exhibits some structure. This is best seen in the data of Figs. 3(b) and 3(c) at $T=3580$ K, for which we have taken more data points. This behavior can be understood from the pair correlation function for the SiSi correlations [Fig. 4(a)]. The comparison of Fig. 4(a) with Figs. 3(b) and 3(c) shows that the locations of shoulders or even maxima in $D_Y$ and Δ are at the locations of

the minima in $g_{SiSi}(r)$. This makes sense because the minima in $g_{SiSi}(r)$ correspond to distances of SiSi pairs that are relatively unlikely and so around these distances the change in the effective screening is weaker than for separations of SiSi pairs at which strong structural correlations occur.

The pair correlation function $g_{SiSi}(r)$ in Fig. 4(b) exhibits a similar behavior as in the case of the Wolf method, although the convergence toward the Ewald result is slower than for the Wolf method. For interparticle distances $r>4$ Å, relatively strong deviations from the Ewald result can be observed for $r_c=6.0$ Å. Note that the first peak in $g_{SiSi}(r)$ which is not shown in Fig. 4(b) is also well reproduced for $r_c=6.0$ Å. For $r_c=10.17$ Å, the agreement with the Ewald result extends to the second peak in $g_{SiSi}(r)$, while for interparticle distances $r>7$ Å, the Yukawa result is out of phase with respect to the Ewald result.

The dynamic properties of the Yukawa potentials are represented in Fig. 4(b) by the mean-squared displacement $\langle r_\alpha^2(t)\rangle$ for the oxygen particles (i.e., $\alpha$=O) at the temperatures $T=6100$ and 3250 K, defined by

$$\langle r_\alpha^2(t)\rangle = \left\langle \frac{1}{N_\alpha}\sum_{i=1}^{N_\alpha} |\mathbf{r}_i(t)-\mathbf{r}_i(0)|^2 \right\rangle. \tag{10}$$

We find similar results for Si atoms. For different values of $r_c$, a similar qualitative behavior at the high and the low temperature is seen, albeit effects are more pronounced at the low temperature. In the diffusive regime, the dynamics becomes faster when decreasing the cutoff $r_c$. Thus, as in the case of the Wolf method, a change in long-range structural correlations is accompanied by a faster diffusion of the particles. In the next section, we present more extensive results for $r_c=10.17$ Å for the Yukawa potential. This cutoff provides a reasonable accuracy compared to the Ewald results, although the agreement cannot be made as good as the Wolf case for the same cutoff value.

The simulations with the Yukawa potential (also those shown in Fig. 4) were done for systems of 1152 particles at a total mass density of 2.37 g/cm$^3$, i.e., the same density that we also used for the simulations in which the Ewald sums and those in which the Wolf method was applied. Furthermore the results presented in the next section have been obtained considering average values for the Yukawa parameters, i.e., $D_Y=1.07$ and $\Delta=5.649$ Å.

## III. DETAILED COMPARISON WITH THE LONG-RANGE MODEL

In this section, we present a detailed comparison of the static and dynamic behavior of the Wolf and Yukawa finite-range potentials for liquid silica and the one obtained with Ewald summation using parameters described in the previous section.

### A. Static properties

In Fig. 5, we show the static pair correlation functions for Si–Si, O–O, and Si–O pairs at a single, low temperature, $T=3000$ K. At first sight, it is obvious that there is a fairly good agreement between the three sets of data. Looking at the data more closely, one can see that although short-range structure, $0<r<5$ Å, is well reproduced by the two finite-range potentials, small deviations are present at larger distances, $r>7$ Å, as evidenced in the three insets of Fig. 5. It is interesting that Wolf and Yukawa potentials produce deviations with opposite trends. Wolf data reveal a liquid which is more structured at large distances than in the Ewald simulations, while the Yukawa potential produces less structured pair correlation functions. We do not have a simple physical explanation for this opposite tendency. We also remark that large distance oscillations in the Yukawa potential are slightly out of phase with the Ewald results, as are best seen for the Si–Si correlations [see also Fig. 4(b)]. However, overall, we conclude that the local structure of silica is very well reproduced by the finite-range potentials. Large distance correlations are more sensitive to the truncation of the Coulombic interaction, but reasonable agreement can nevertheless be obtained for the parameters chosen in Sec. II.

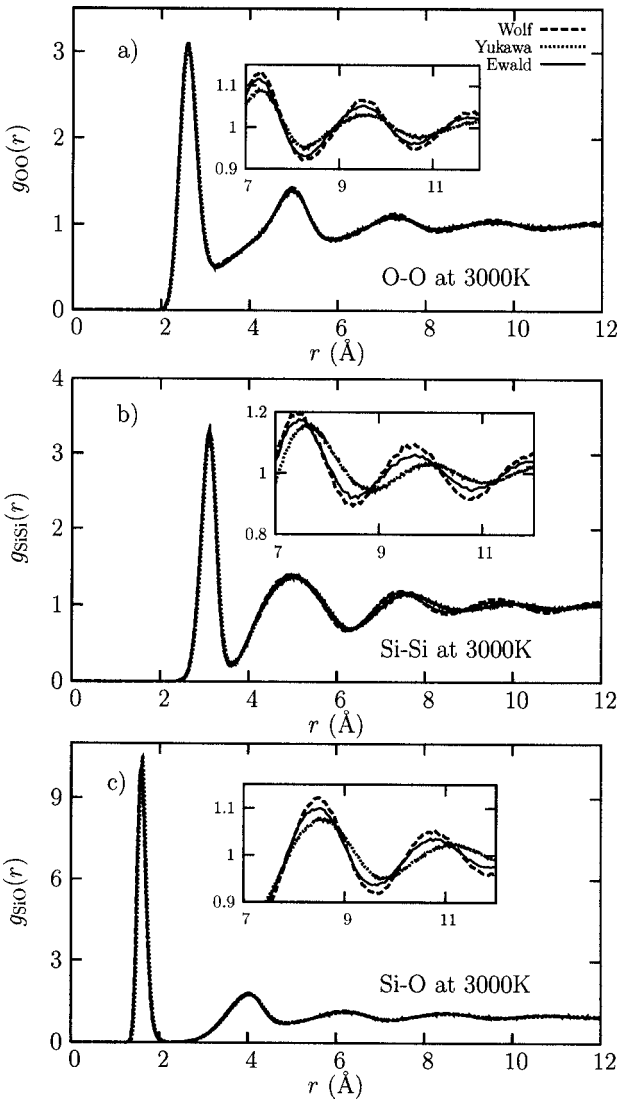


FIG. 5. Static pair correlation functions for Ewald, Wolf, and Yukawa simulations for $T=3000$ K ($r_c=10.17$ Å). The overall structure of the liquid is the same for the three simulations, although small deviations are observed at large distances, as shown in the insets.

The opposite large distance behavior of the Wolf and

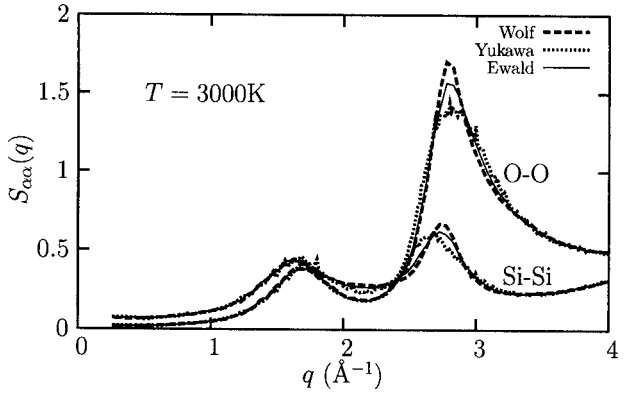


FIG. 6. Partial static structure factor for O–O and Si–Si correlations at $T=3000$ K and for the three simulation methods. The overall structure of the fluid is correct, with small deviations close to the peak at 2.9 Å$^{-1}$.

Yukawa data is also clearly revealed when looking at the partial static structure factors, as shown in Fig. 6. As compared to Ewald simulations, the Wolf data correctly reproduce $S(q)$ for both small ($q<2.5$ Å$^{-1}$) and large ($q>3.5$ Å$^{-1}$) wave vectors, while the height of the peak at $q\approx 2.9$ Å$^{-1}$ is slightly too large. This is consistent with the observation of a large distance structure seen in the pair correlation functions. Similarly, the Yukawa data underestimate the height of this peak, while its position is also slightly incorrect in the case of Si–Si correlations. As discussed in Sec. II, it is important to recall that the amplitudes of these deviations are more pronounced at low temperatures when the fluid is more structured.

The fact that the short-range structure of the fluid is well reproduced by our finite-range potentials is confirmed in Fig. 7 which presents Si–O–Si and O–Si–O bond angle distributions for the three models. We find that at all temperatures the local atomic arrangements are indeed very similar in the three cases. We find similar results for Si–Si–Si angle distributions. This is consistent with the above observation that small differences in the pair correlation functions are only seen at very large distances. These large distance differences do not affect the local tetrahedral arrangement of the atoms.

In Fig. 8, we show the temperature dependence of the pressure $P$. As mentioned above, we find that the pressure is very sensitive to the truncation of the Coulombic interaction. Nevertheless, the agreement between Wolf and Ewald results is very good, while somewhat larger deviations are observed for the Yukawa potential. Again the sign of the deviations is opposite for Wolf and Yukawa results.

### B. Dynamic properties

In Fig. 9, we compare the mean-squared displacements $\langle r_\alpha^2(t)\rangle$ for both Si and O species for several temperatures to the Ewald results. Within the statistical noise, we cannot observe any difference between the Ewald and the Wolf data at the two highest temperatures. For $T=3000$ K, there is a small difference between the two methods on time scales corresponding to thermal vibrations, as discussed in the context of Fig. 2. A similar agreement is found for the mean-squared displacements in Fig. 9, although the use of logarithmic scales somewhat obscures the little differences between the

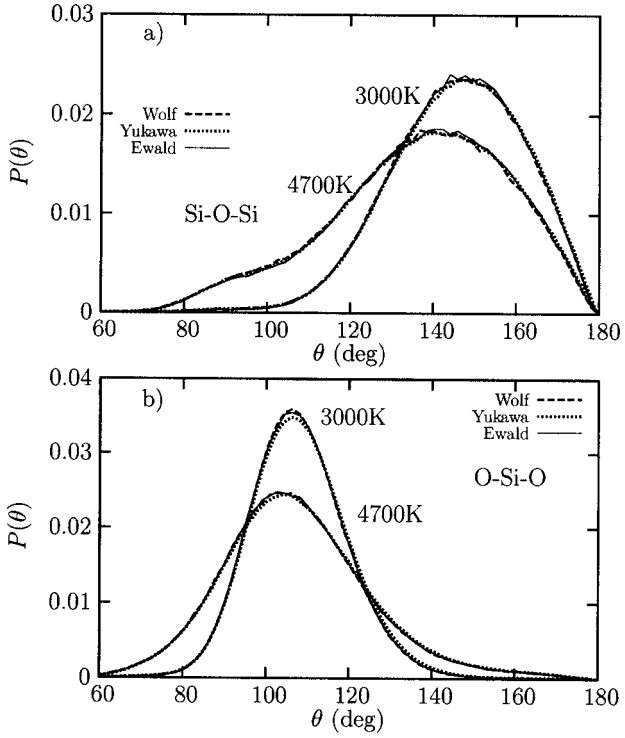


FIG. 7. Bond angle distributions (Si–O–Si and O–Si–O) for two temperatures and for the three simulation methods. The agreement between the three models is very good at all temperatures.

two sets of data. From Fig. 9, we also deduce that the temperature evolution of the relaxation time scales and diffusion constants is similar using both Wolf and Ewald methods. It is striking that despite the small differences in the structure of Ewald and Wolf data, their dynamical behavior is in excellent agreement. This is not true for the Yukawa potential where larger deviations can be noticed in Fig. 9.

The Yukawa data in Fig. 9 also imply that dynamic properties of the Yukawa and the Ewald models have a slightly different temperature evolution. This can be illustrated by the temperature dependence of the self-diffusion constants. We have calculated the self-diffusion constants $D_\alpha$ via the long-time limit of the mean-squared displacements using the Einstein relation,

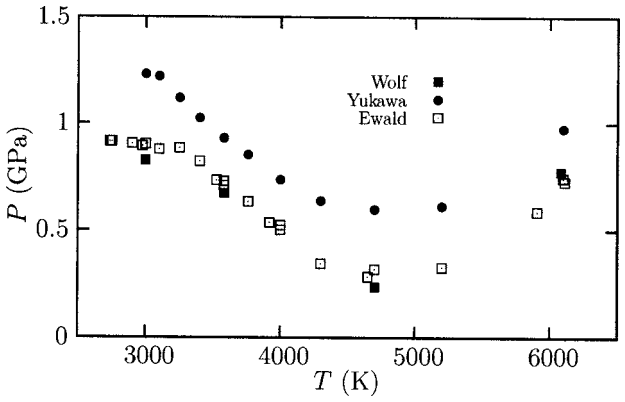


FIG. 8. Temperature dependence of the pressure for the three potentials.

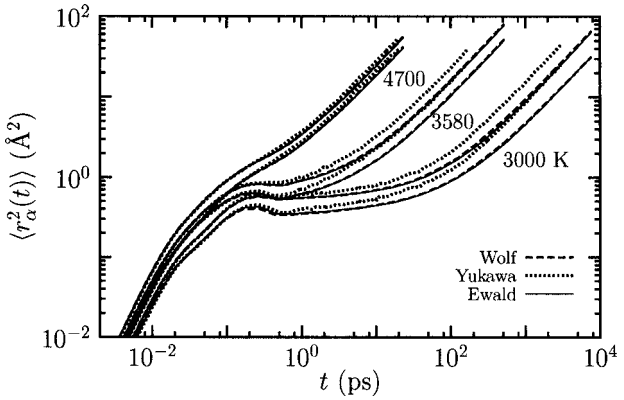


FIG. 9. Mean-squared displacements for the three simulation techniques at three different temperatures. At each temperature we show both the Si and O dynamics, the latter being the fastest. The agreement between Wolf and Ewald is excellent. The slowing down of the dynamics of the Yukawa potential is slightly less pronounced.

$$D_\alpha = \lim_{t\to\infty} \frac{\langle r_\alpha^2(t)\rangle}{6t}. \tag{11}$$

Figure 10 displays the diffusion constants in an Arrhenius plot. Note that we do not plot the Wolf results in this figure because there are only minor differences between Wolf and Ewald data in the full temperature range. Whereas at the highest temperature, $T=6100$ K, Yukawa and Ewald methods yield the same values for $D_\alpha$ within the statistical accuracy, and at lower temperatures, the Yukawa values are a factor of 2–3 higher than the "exact" Ewald values. Note that at low temperatures the Yukawa result for $D_{\mathrm{Si}}$ coincides with the Ewald result for $D_{\mathrm{O}}$. This is certainly a coincidence but it illustrates that qualitatively, the temperature dependence as obtained from the Yukawa potential is very similar to that of the exact calculation with Ewald sums. In particular, from both methods, similar activation energies are expected for the temperature dependence of $D_\alpha$ in the low-temperature regime.

Finally, we show in Fig. 11 that the vibrational density of states $g(\nu)$ is well reproduced by the Wolf method and, on a qualitative level, also by the Yukawa method. In order to compute $g(\nu)$, we quenched ten independent liquid samples with an infinite cooling rate, i.e., a steepest descent, down to

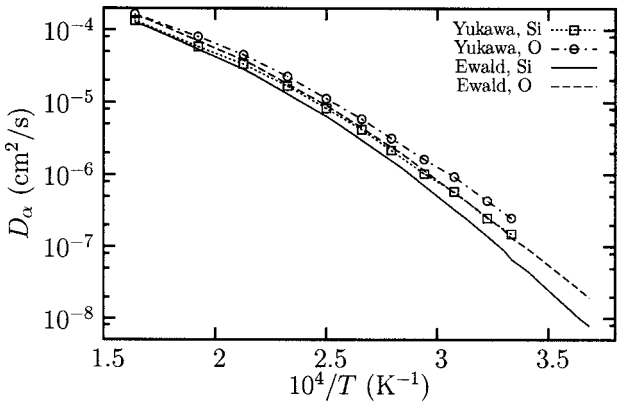


FIG. 10. Arrhenius plots of the self-diffusion constants for Ewald and Yukawa methods.

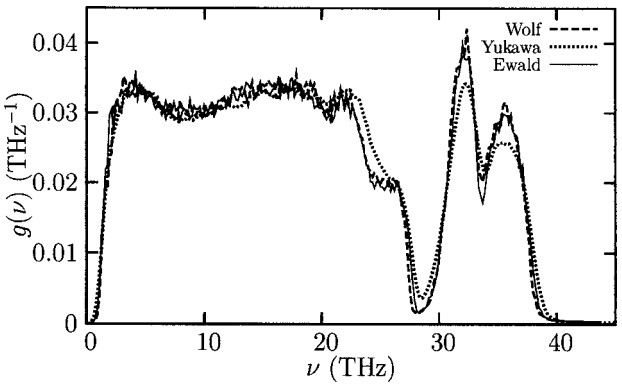


FIG. 11. Vibrational density of states for the three potentials.

$T=300$ K, followed by an annealing during 80 ps. We then measured the velocity autocorrelation function and obtained $g(\nu)$ from its Fourier transform.[46] The liquid starting configurations were well-equilibrated samples at $T=2715$ K for the Ewald as well as the Wolf case and at $T=3000$ K for the Yukawa case. As we see in Fig. 11, Ewald and Wolf results for $g(\nu)$ are in very good agreement, while the Yukawa method yields slight deviations from the Ewald calculations, in particular, at high frequencies ($\nu>30$ THz) where $g(\nu)$ exhibits a double-peak structure. The latter peaks are due to intertetrahedral stretching modes. In the past, it has been shown that cooling rate effects affect especially the amplitude of the high-frequency peaks.[2,5] Thus, part of the deviations seen in the Yukawa results might be due to the different cooling history that we used for the Yukawa case. We also mention that in the frequency range of 5 THz$\leqslant\nu\leqslant$25 THz, the vibrational dynamics in the BKS model is quite unrealistic, as has been revealed by the comparison with Car-Parrinello MD simulations.[13] The results of the present study suggest that an improvement of the BKS model with respect to vibrational properties can be also achieved by a finite-range potential.

## IV. CONCLUSION

Extensive MD simulations have been used to study finite-range approximations of the BKS model for silica. We have demonstrated that both the Wolf method and a screened Coulomb (Yukawa) potential can be used to approximate the Coulomb interactions in BKS silica. In order to obtain a quantitative agreement with Ewald sums, a cutoff of about 10 Å has to be used for the Wolf potential. Such a potential cannot be classified as a short-range potential since its spatial extent corresponds to about three connected $SiO_4$ tetrahedra. However, due to its finite range, the Wolf potential can be efficiently applied to problems where Ewald sums become inefficient, such as quasi-two-dimensional geometries, MC simulations,[24,25] or MD simulations with a very large number of particles. In the case of the Yukawa potential, larger cutoffs have to be used to yield a quantitative agreement with Ewald results. However, we have to keep in mind that we have simply reparametrized the Coulomb interaction term of the BKS model. An interesting possibility would be to per-

form a more complete reparametrization of the BKS potential, so that a smaller cutoff value could be used, making simulations even more efficient.

## ACKNOWLEDGMENTS

The authors are grateful to K. Binder and D. Reichman for stimulating discussions. They gratefully acknowledge financial support by Schott Glas and computing time on the JUMP at the NIC Jülich, and on IBM/SP at CINES in Montpellier. One of the authors (L.B.) is partially funded by the Joint Theory Institute at the Argonne National Laboratory and the University of Chicago.

[1] P. H. Poole, P. F. McMillan, and G. H. Wolf, Rev. Mineral. **32**, 563 (1995).
[2] K. Vollmayr, W. Kob, and K. Binder, Phys. Rev. B **54**, 15808 (1996).
[3] S. N. Taraskin and S. R. Elliott, Europhys. Lett. **39**, 37 (1997); Phys. Rev. B **56**, 8605 (1997).
[4] J. Horbach and W. Kob, Phys. Rev. B **60**, 3169 (1999).
[5] J. Horbach, W. Kob, and K. Binder, J. Phys. Chem. B **103**, 4104 (1999).
[6] M. Benoit, S. Ispas, P. Jund, and R. Jullien, Eur. Phys. J. B **13**, 631 (2000).
[7] J. Horbach, W. Kob, and K. Binder, Eur. Phys. J. B **19**, 531 (2001).
[8] P. Scheidler, W. Kob, A. Latz, J. Horbach, and K. Binder, Phys. Rev. B **63**, 104204 (2001).
[9] A. Roder, W. Kob, and K. Binder, J. Chem. Phys. **114**, 7602 (2001).
[10] M. H. Müser and K. Binder, Phys. Chem. Miner. **28**, 746 (2001).
[11] I. Saika-Voivod, F. Sciortino, and P. H. Poole, Phys. Rev. E **63**, 011202 (2001).
[12] J. Horbach and K. Binder, J. Chem. Phys. **117**, 10796 (2002).
[13] M. Benoit and W. Kob, Europhys. Lett. **60**, 269 (2002).
[14] I. Saika-Voivod, F. Sciortino, and P. H. Poole, Phys. Rev. E **69**, 041503 (2004).
[15] I. Saika-Voivod, F. Sciortino, T. Grande, and P. H. Poole, Phys. Rev. E **70**, 061507 (2004).
[16] M. S. Shell, P. G. Debenedetti, and A. Z. Panagiotopoulos, Phys. Rev. E **66**, 011202 (2002).
[17] A. Saksaengwijit, J. Reinisch, and A. Heuer, Phys. Rev. Lett. **93**, 235701 (2004); A. Saksaengwijit and A. Heuer, Phys. Rev. E **73**, 061503 (2006); **74**, 051502 (2006).
[18] D. Herzbach, K. Binder, and M. H. Müser, J. Chem. Phys. **123**, 124711 (2005).
[19] Y. Ma and S. H. Garofalini, Mol. Simul. **31**, 739 (2005); Phys. Rev. B **73**, 174109 (2006).
[20] A. Kerrache, V. Teboul, and A. Monteil, Chem. Phys. **321**, 69 (2006).
[21] F. Léonforte, A. Tanguy, J. P. Wittmer, and J.-L. Barrat, Phys. Rev. Lett. **97**, 055501 (2006).
[22] Y. F. Liang, C. R. Miranda, and S. Scandolo, J. Chem. Phys. **125**, 194524 (2006); Phys. Rev. B **75**, 024205 (2007).
[23] L. Berthier, G. Biroli, J.-P. Bouchaud, W. Kob, K. Miyazaki, and D. Reichman, J. Chem. Phys. **126**, 184503 (2007); **126**, 184504 (2007).
[24] L. Berthier, Phys. Rev. E **76**, 011507 (2007).
[25] L. Berthier, Phys. Rev. Lett. **98**, 220601 (2007).
[26] B. W. H. van Beest, G. J. Kramer, and R. A. van Santen, Phys. Rev. Lett. **64**, 1955 (1990).
[27] P. P. Ewald, Ann. Phys. **64**, 253 (1921).
[28] M. Allen and D. Tildesley, *Computer Simulation of Liquids* (Oxford University Press, Oxford, 1987).
[29] D. Frenkel and B. Smit, *Understanding Molecular Simulation* (Academic, London, 2002).
[30] J. Perram, H. G. Petersen, and S. de Leeuw, Mol. Phys. **65**, 875 (1988).
[31] D. E. Parry, Surf. Sci. **49**, 433 (1975); **54**, 195 (1976).
[32] R. W. Hockney and J. W. Eastwood, *Computer Simulation Using Particles* (IOP, London, 1988).
[33] M. Deserno and C. Holm, J. Chem. Phys. **109**, 7678 (1998); **109**, 7694 (1998).
[34] A. Arnold, J. de Joannis, and C. Holm, J. Chem. Phys. **117**, 2496 (2002); J. de Joannis, A. Arnold, and C. Holm, J. Chem. Phys. **117**, 2503 (2002).
[35] L. Greengard and V. Rhoklin, J. Comput. Phys. **73**, 325 (1987).
[36] K. Esselink, Comput. Phys. Commun. **87**, 375 (1995).
[37] D. Wolf, Phys. Rev. Lett. **68**, 3315 (1992).
[38] D. Wolf, P. Keblinski, S. R. Phillpot, and J. Eggebrecht, J. Chem. Phys. **110**, 8254 (1999).
[39] C. J. Fennell and J. D. Gezelter, J. Chem. Phys. **124**, 234104 (2006).
[40] P. Gallo, M. Rovere, and E. Spohr, Phys. Rev. Lett. **85**, 4317 (2000); J. Chem. Phys. **113**, 11324 (2000).
[41] C. Avendano and A. Gil-Villegas, Mol. Phys. **104**, 1475 (2006).
[42] J. A. Moreno-Razo, E. Diaz-Herrera, and S. H. L. Klapp, Mol. Phys. **104**, 2841 (2006).
[43] K. Binder and W. Kob, *Glassy Materials and Disordered Solids: An Introduction to Their Statistical Mechanics* (World Scientific, London, 2005).
[44] D. Zahn, B. Schilling, and S. M. Kast, J. Phys. Chem. B **106**, 10725 (2002).
[45] W. H. Press, S. A. Teukolksy, W. T. Vetterling, and B. P. Flannery, *Numerical Recipes in Fortran 77: The Art of Scientific Computing* (Cambridge University Press, Cambridge, 1992), Vol. 1.
[46] M. T. Dove, *Introduction to Lattice Dynamics* (Cambridge University Press, Cambridge, 1993).